Supplementary Information

Novel 1,8-Naphthalimide derivative with an open space for an anion: Unique fluorescence behaviour depending on the anion's electrophilic property

Hironori Izawa,*[,a] Shoji Nishino, [a] Masato Sumita,*[,b] Masaaki Akamatsu,[c] Kenji Morihashi,[d] Shinsuke Ifuku,[a] Minoru Morimoto,[a] and Hiroyuki Saimoto[a]

[a] Graduate School of Engineering, Tottori University, 4-101 Koyama-Minami, Tottori 680-8550, Japan.

[b] National Institute for Materials Science (NIMS), 1-1 Namiki, Tsukuba, Ibaraki 305-0044, Japan.

[c] Department of Pure and Applied Chemistry, Tokyo University of Science, 2641 Yamazaki, Noda, Chiba 278-8510, Japan.

[d] Department of Chemistry, University of Tsukuba, 1-1-1 Tennoudai, Ibaraki 305-8571, Japan.

1. Materials and methods

Materials 1, 8-Naphthalic anhydride and 1-methylimidazole was purchased from Sigma-Aldrich Japan (Tokyo, Japan). 2-Chloroethylamine hydrochloride and Sodium dicyanamide was purchased from Tokyo Chemical Industry Co., Ltd. (Tokyo, Japan). Sodium fluoride, sodium chloride, sodium bromide, sodium iodide and sodium acetate were purchased from Wako Pure Chemical Industries Ltd. (Osaka, Japan). Sodium thiocyanate, sodium dihydrogenphosphate, and sodium hydroxide were purchased from Nacalai Tesque, Inc (Tokyo, Japan). *N*-(2-Chloroethyl)-1,8-naphthalimide and was synthesized in accordance with previously reported procedure[1]. Other reagents were used as commercial grade without further purification.

Instruments NMR spectra were obtained using an JNM-ECX500 spectrophotometer (JEOL). Mass spectra were measured using an Exactive^{TM} plus Orbitrap MASS spectrometer (Thermo Fischer SCIENTIFIC). IR spectra were obtained using a Spectrum 65 (Perkin Elmer). Elemental analysis data were recorded on a Perkin Elmer 2400 II CHNS/O. UV-Vis spectra were recorded on a Jasco V-550 spectrophotometer (Shimadzu). Fluorescence spectra were recorded on a SHIMADZU RF-5300PC (Shimadzu). Quantum yields were recorded on a C9920-02 (Hamamatsu Photonics).

Synthesis of 1-Methyl-3-(*N*-(1,8-naphthalimidyl)ethyl)imidazolium chloride (MNEI-Cl)

N-(2-Chloroethyl)-1,8-naphthalimide (0.768 g, 2.958 mmol) and 1-methylimidazole (1.007 g, 12.264 mmol) was added to DMF (20 mL) and stirred at 120 ^{o}C for 3 days. After cooling, DMF was removed under reduced pressure, and the residue was washed with ethylacetate. The precipitate was collected by filtration, followed by washed with large amount of ethylacetate, and dried under reduced pressure to give product (0.3271 g, 0.9091

mmol) in 30.7 % yield. ^{1}H NMR (500 MHz, D_2O, DSS) δ = 3.67 (s, 3H, C*H*$_3$-), 4.38 (t, 2H, *J* = 10 Hz, -CH_2C*H*$_2$-), 4.43 (t, 2H, J = 10 Hz, -CH_2C*H*$_2$-), 7.21 (s, 1H, -*H*C=CH- in imidazole), 7.34 (s, 1H, -*H*C=CH- in imidazole), 7.63 (t, 2H, *J* = 15 Hz, Naphthalimide), 8.21 (d, 2H, *J* = 20 Hz, Naphthalimide) , 8.24 (d, 2H, *J* = 20 Hz, Naphthalimide), 8.63 (s, 1H, -N-*H*C=N- in imidazole) ppm. ^{13}C NMR (125 Hz, D_2O, DSS). δ = 36.19, 40.49, 47.80, 120.09, 123.29, 124.19, 127.07, 127.54, 131.21, 132.11, 136.09, 136.90, 165.07 ppm. ESI-MS : *m*/*z*: 306.12 $[MNEI]^+$. Elemental analysis calcd. for $(C_{18}H_{16}ClN_3O_2)_3 \cdot (H_2O)_4$ C 59.10 H 5.14 N 11.49, found C 59.10 H 5.16 N 11.66.

2.Excitation spectra of MNEI-Cl aqueous solution

Figure S1 shows excitation spectra of 0.07-2.90 mM MNEI-Cl aqueous solution. Interestingly, the spectra are drastically varied in concentration. Excitation spectra of 0.07 mM solution show good correlation with its UV-vis spectrum, whereas it is not shown at concentration higher than 0.29 mM. These results suggest the formation of the aggregate higher than 0.29 mM.

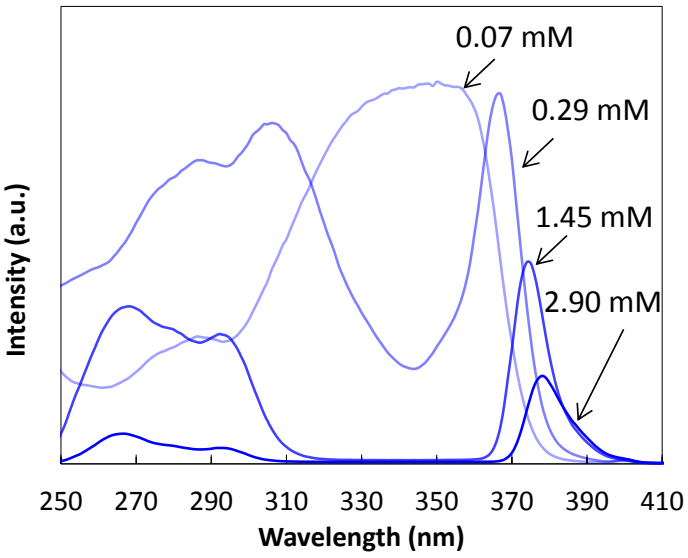

Fig. S1. Fluorescence excitation spectra of 0.07-2.90 mM MNEI-Cl in water.

3. ^{1}H NMR analysis of MNEI in NaOD/D_2O solution

Figure S2 shows ^{1}H NMR spectrum of 1.45 mM MNEI in 210 mM NaOD-D_2O solution. The signals attributed to the hydrolyzed MNEI are shown. Note that the proton **j** in the imidazolium group is completely replaced with deuterium because of the carbene formation in the presence of a base.[2]

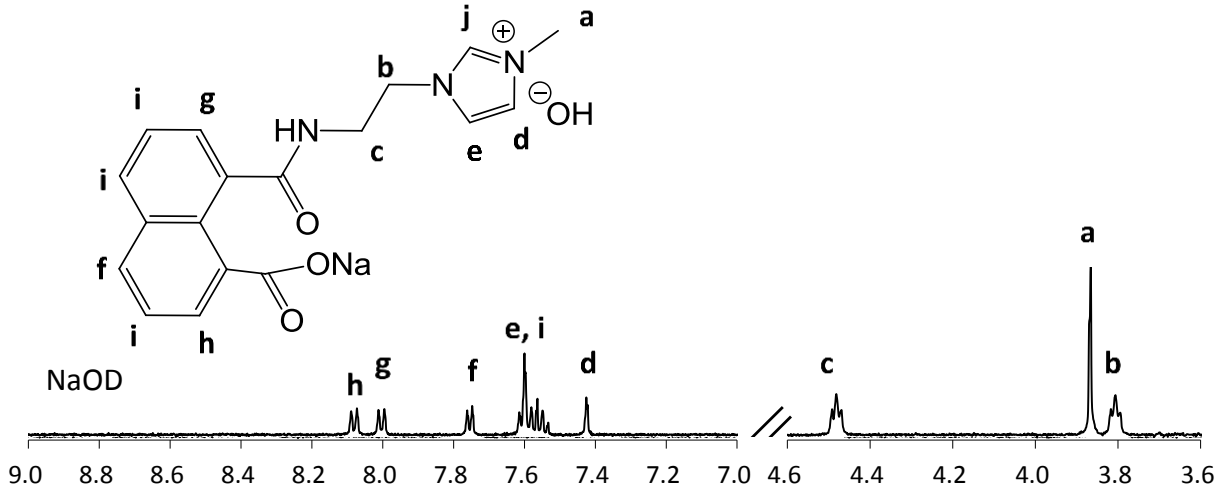

Fig. S2. ^{1}H NMR spectrum of 1.45 mM MNEI-Cl in 210 mM NaOD/D_2O solution

4. Correlations between fluorescence intensity of MNEI solution and pH and atomic radius

There is no correlation with the pH. In the atomic radius[3], smaller atom show higher fluorescence intensity. However, this do not apply to SCN^- and $N(CN)_2^-$.

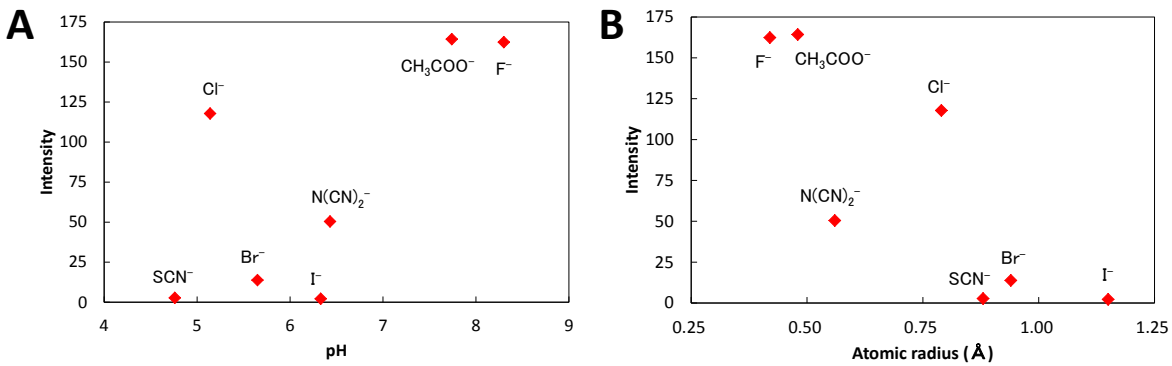

Fig. S3. Correlations between fluoresence intensity of 1.45 mM MNEI solution and pH of the solution (A), atomic radius (B).

5. ^{1}H NMR spectrum of MNEI in the presence of NaF and NaBr

Figure S4 shows ^{1}H NMR analyses of 1.45 mM MNEI in 210 mM NaF/D_2O and NaI/D_2O. There is no difference in the spectra.

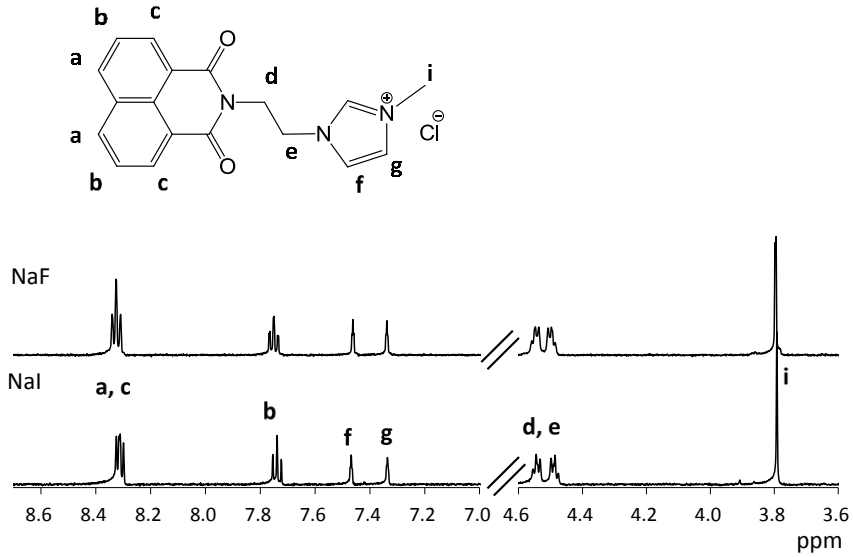

Fig. S4. ^{1}H NMR spectra of 1.45 mM MNEI in 210 mM NaF/D_2O and NaI/D_2O.

6. Stern-volmer plot of the MNEI-Cl-NaCl sysetem

The fluorescence spectra of the 1.45 mM MNEI-Cl in the presence of salt (Fig. S6) was applied to Stern-volmer plot.

$$\frac{F_0}{F} = 1 + K[NaCl] \qquad (1)$$

, where F, F_0, and K are the fluorescence intensity at 400 nm or 480 nm of MNEI-Cl solution in the presence and absence of NaCl, respectively, and a stern-volmer constant.

7. Computation details

All calculations were performed by using density functional theory with B3LYP functional implemented in GAUSSIN09[5]. Vertically excited energy of twenty lowest excited states were estimated by using time dependent strategy (TD-DFT) with the same functional. 6-31G* basis set is used except for Iodine. DGDZVP effective core potential basis set was applied to Iodine.

In each MNEI complex, vertically excited energies, leading configuration, and the values of oscillator strength are tabulated in Table S1-S5. Orbitals, which related to the excited states of each specie, are also shown in Figure S5-S9.

We have also checked that the qualitative results at the B3LYP/6-31G* level is enough to design this system by performing the calculation with CAM-B3LYP functional or 6-31G*/6-31+G* basis sets. The results are tabulated in Table S7-S13 and S_{M1} , CT_0, and CT_1 as the function of electronegativity at each level are shown in Figure S10.

7-1. MNEI *in vacuo*

Table S1. Vertical excited energy (Ev) and Oscillator strength (OS)

State	Configuration	Ev / eV	OS
S_1	HOMO/LUMO	3.6411 (340.51 nm)	0.2273
S_2	HOMO-1/LUMO+1 HOMO/LUMO+4	3.9464 (314.17 nm)	0.0413

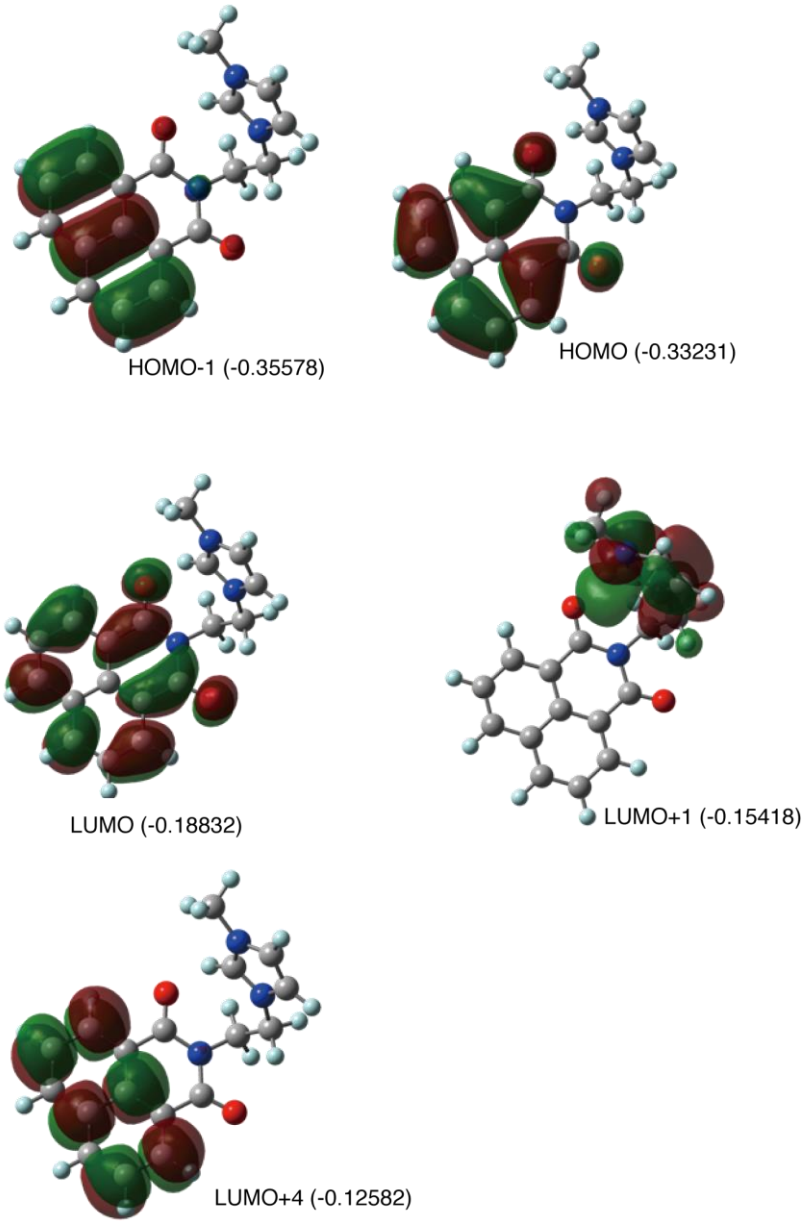

Fig. S5. Orbitals and their energies (in E_h) which related to excited state of MNEI in *vacuo*.

7-2. MNEI + F^-

Table S2. Vertical excited energy (Ev) and oscillator strength (OS)

State	Configuration	Ev / eV	OS
S_1	HOMO/LUMO (49%)	1.7159 (722.55 nm)	0.0028
S_2	HOMO/LUMO+1 (5.7%)	3.4108 (363.50 nm)	0.0006
	HOMO/LUMO+2 (44%)		
S_3	HOMO/LUMO+1 (44%)	3.4627 (358.05 nm)	0.0000
	HOMO/LUMO+2 (5.7%)		
S_4	HOMO-4/LUMO (1.8%)	3.6970 (335.36 nm)	0.0000
	HOMO-3/LUMO (39.6%)		
	HOMO-2/LUMO (4.2%)		
	HOMO-1/LUMO (2.4%)		
S_5	HOMO-3/LUMO (2.4%)	3.7470 (330.89 nm)	0.1923
	HOMO-1/LUMO+1 (46%)		
S_6	HOMO-6/LUMO (2.6%)	3.8822 (319.37 nm)	0.0014
	HOMO-3/LUMO (5%)		
	HOMO-2/LUMO (40%)		
S_7	HOMO-4/LUMO (40%)	4.0691 (304.70 nm)	0.0184
	HOMO-2/LUMO (1.3%)		
	HOMO-1/LUMO+1 (6.3%)		
S_8	HOMO-6/LUMO (40.8%)	4.2095 (294.53 nm)	0.0000
	HOMO-5/LUMO (2.3%)		
	HOMO-3/LUMO+2 (1.9%)		
	HOMO-2/LUMO (3.6%)		
S_9	HOMO/LUMO+3 (50%)	4.3666 (283.94 nm)	0.0008

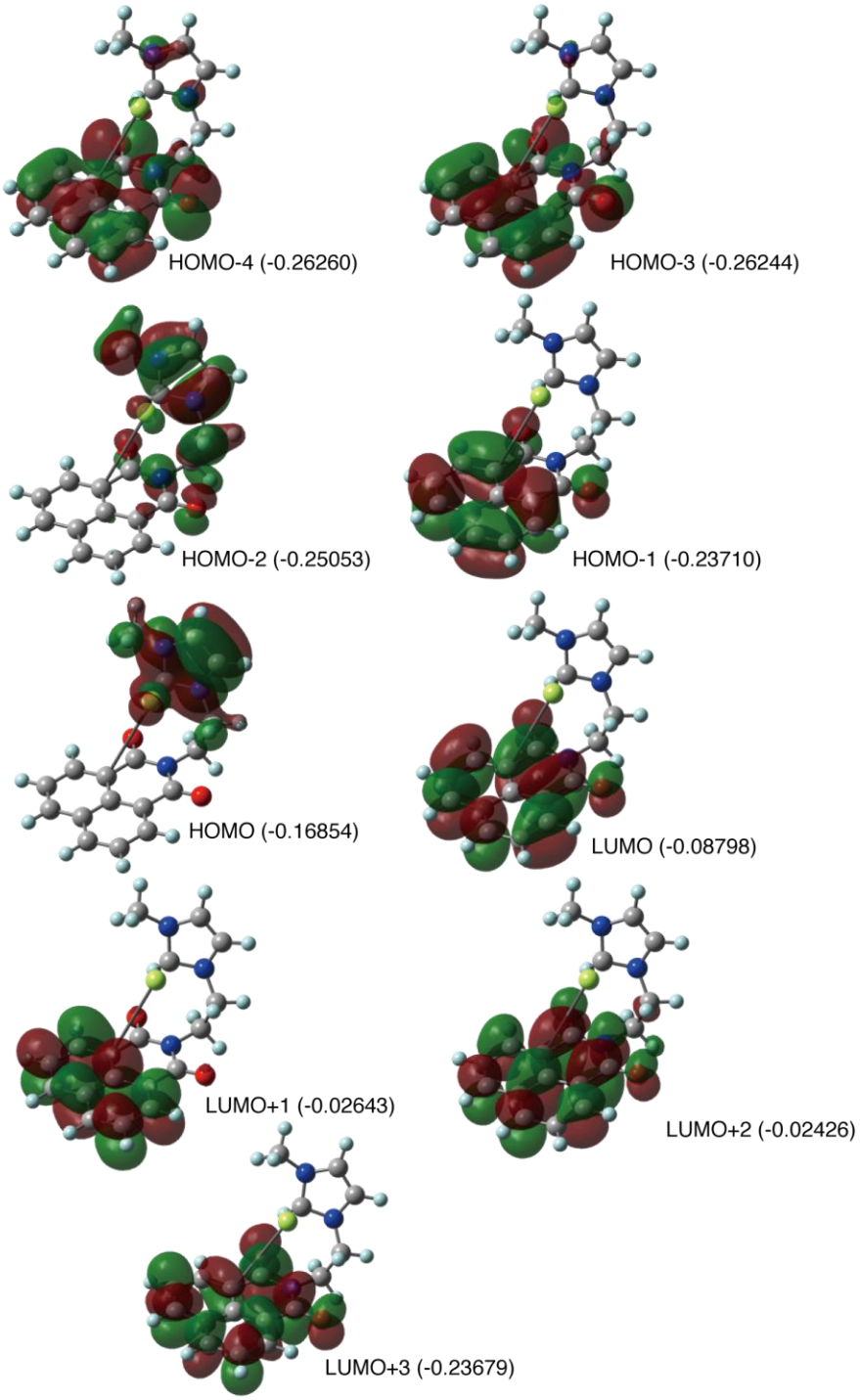

Fig. S6. Orbitals and their energies in E_h which related to excited state of MNEI-F anion in *vacuo*.

7-3. MNEI + Cl^-

Table S3. Vertical excited energy (Ev) and oscillator strength (OS)

State	Configuration	Ev / eV	OS
S_1	HOMO/LUMO (47%)	2.1196 (584.93 nm)	0.0024
	HOMO-1/LUMO (2%)		
S_2	HOMO-1/LUMO (47%)	2.1749 (570.08 nm)	0.0114
	HOMO/LUMO (2%)		
S_3	HOMO-2/LUMO (49%)	2.2197 (558.56 nm)	0.0002
S_4	HOMO-3/LUMO+1 (34%)	3.7306 (332.34 nm)	0.1803
S_5	HOMO/LUMO+1 (48.4%)	3.7814 (327.88 nm)	0.0066
S_6	HOMO-1/LUMO+1 (45%)	3.8107 (325.35 nm)	0.0189
	HOMO-1/LUMO+3 (3%)		

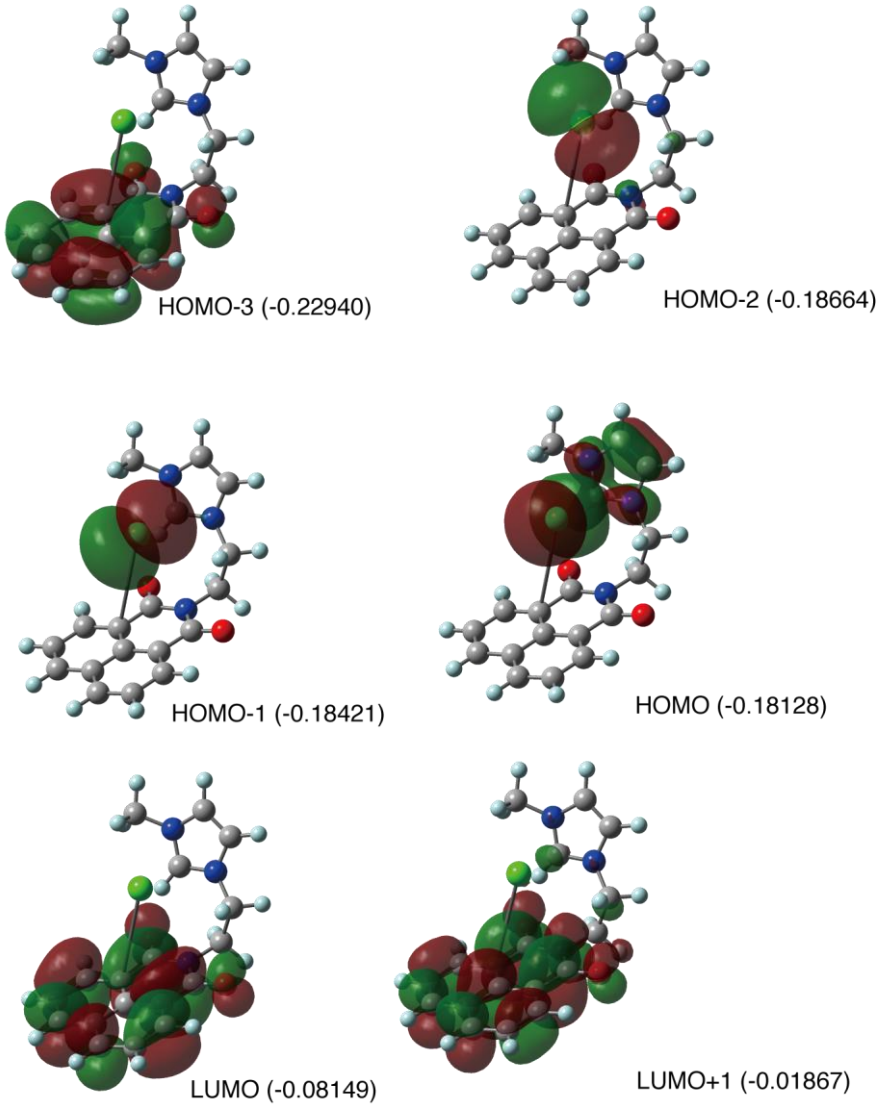

Fig. S7. Orbitals and their energies in E_h which related to excited state of MNEI-Cl anion in *vacuo*.

7-4. MNEI + Br^-

Table S4. Vertical excited energy (Ev) and oscillator strength (OS)

State	Configuration	Ev / eV	OS
S_1	HOMO/LUMO (2%)	1.9975 (620.69 nm)	0.0019
	HOMO-1/LUMO (47%)		
S_2	HOMO-2/LUMO (7.9%)	2.0207 (613.56 nm)	0.0167
	HOMO-1/LUMO (1.4%)		
	HOMO/LUMO (41%)		
S_3	HOMO-2/LUMO (42%)	2.0504 (604.68 nm)	0.0031
	HOMO-1/LUMO (1.7%)		
	HOMO/LUMO (6.7%)		
S_4	HOMO-1/LUMO+1 (34%)	3.6268 (341.85 nm)	0.0053
	HOMO-1/LUMO+3 (7%)		
	HOMO/LUMO+1 (6%)		
S_5	HOMO-1/LUMO+1 (39%)	3.6702 (337.81 nm)	0.0047
	HOMO/LUMO+1 (9%)		
S_6	HOMO-3/LUMO (2.4%)	3.6938 (335.65 nm)	0.0036
	HOMO-1/LUMO+1 (46%)		
S_7	HOMO-3/LUMO (40%)	3.7308 (332.32 nm)	0.1475
	HOMO-1/LUMO+2 (1%)		
	HOMO-1/LUMO+3 (3%)		
	HOMO/LUMO+3 (2%)		

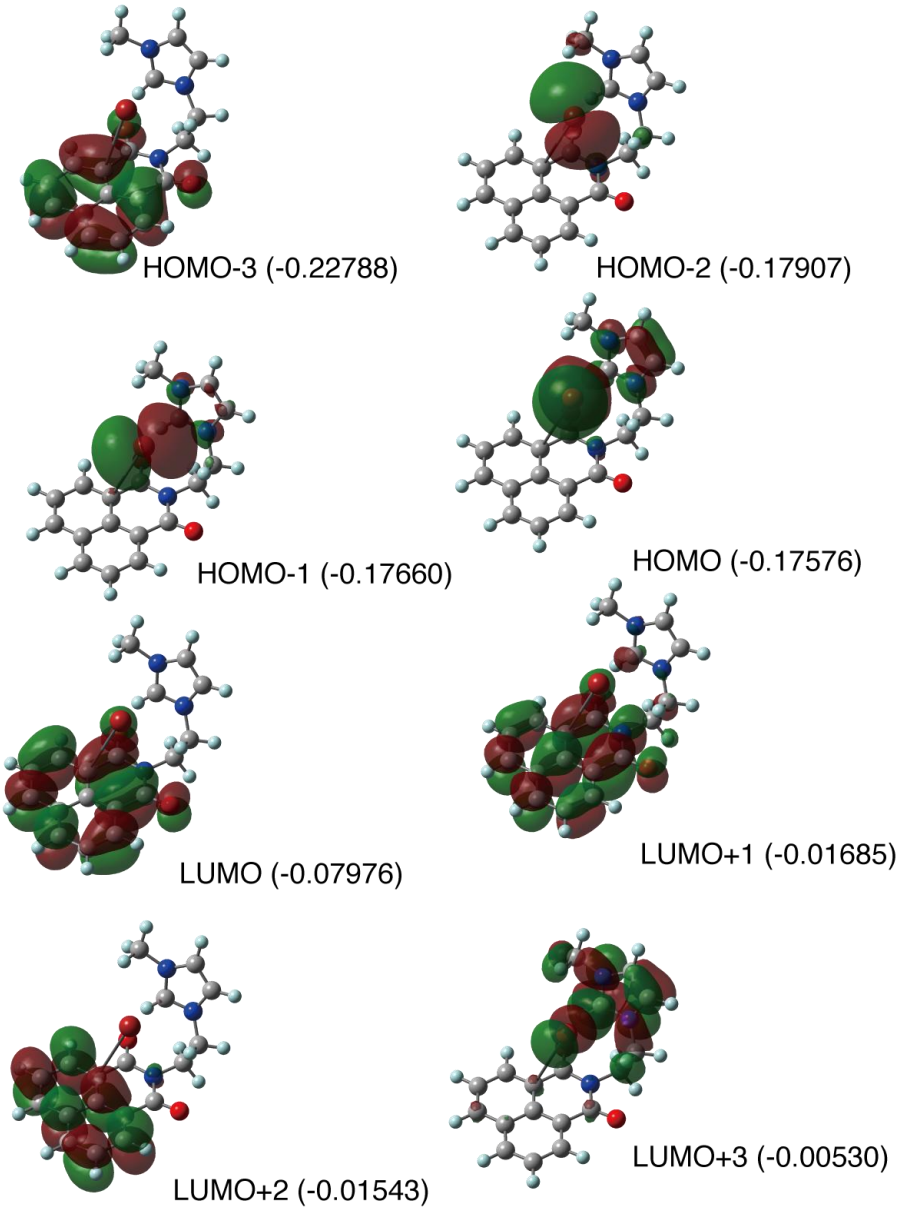

Fig. S8. Orbitals and their energies in E_h which related to excited state of MNEI-Br anion in *vacuo*.

7-5. MNEI + I^-

Table S5. Vertical excited energy (Ev) and oscillator strength (OS)

State	Configuration	Ev / eV	OS
S_1	HOMO/LUMO (49%)	1.6083 (770.91 nm)	0.0026
S_2	HOMO-1/LUMO (49%)	1.6714 (741.79 nm)	0.0002
S_3	HOMO-2/LUMO (49%)	1.7108 (724.71 nm)	0.0020
S_4	HOMO/LUMO+1 (26%)	3.1498 (393.63 nm)	0.0006
	HOMO/LUMO+3 (22%)		
S_5	HOMO-1/LUMO+1 (26%)	3.2052 (386.82 nm)	0.0015
	HOMO-1/LUMO+3 (23%)		

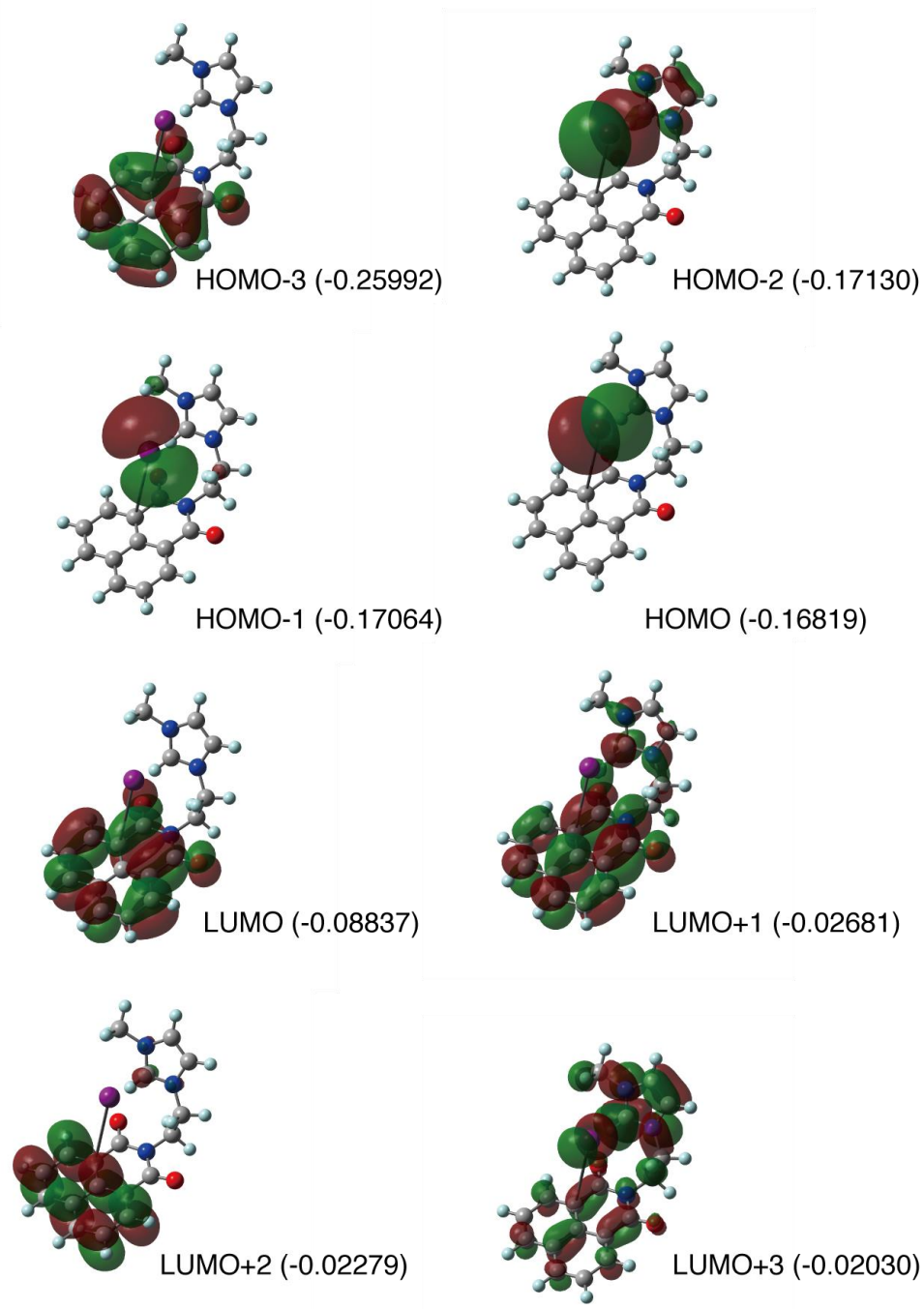

Fig. S9. Orbitals and their energies in E_h which related to excited state of MNEI-I anion in *vacuo*.

Table S6. Relative anion HOMO and MNEI LUMO orbital energy to HOMO of MNEI in eV at the B3LYP/6-31G*

	Only MNEI	Carboxylic anion	F anion	Cl anion	Br anion	I anion
MNEI HOMO	0	0	0	0	0	0
MNEI LUMO	3.91	4.06	4.06	4.02	4.03	4.67
Anion HOMO	_____	1.31	1.87	1.31	1.42	2.50

7-6. Functional and basis set dependence in excited states.

Table S7. Excited energy to S_{M1} state of each MNEI and complex at the several levels.

S_{M1}	B3LYP		CAM-B3LYP	
	6-31G* / eV	6-31+G* / eV	6-31G*	6-31+G*
MNEI	3.641 (340.51 nm)	3.5636 (347.92 nm)	4.0437 (306.61 nm)	3.8238 (324.24 nm)
MNEI+F	3.7470 (330.89 nm)	3.6699 (337.84 nm)	4.1847 (296.28 nm)	4.0760 (304.18 nm)
MNEI+Cl	3.7306 (332.34 nm)	3.6478 (339.88 nm)	4.1574 (298.22 nm)	4.0464 (306.41 nm)
MNEI+Br	3.7308 (332.32 nm)	3.6156 (342.91 nm)	4.1592 (298.10 nm)	4.0463 (306.42 nm)
MNEI+I	3.7259 (332.76 nm)	3.6303 (341.52 nm)	4.1179 (301.09 nm)	4.0090 (309.26 nm)

Table S8. Excited energies to CT_0 states of each complex at the several levels

CT_1	B3LYP		CAM-B3LYP	
	6-31G* / eV	6-31+G* / eV	6-31G*	6-31+G*
MNEI	–––––	–––––	–––––	–––––
MNEI+F	3.4108 (363.50 nm)	3.4447 (359.93 nm)	3.3464 (370.50 nm)	3.3661 (368.34 nm)
MNEI+Cl	2.1196 (584.93 nm)	2.2501 (551.01 nm)	3.3431 (370.87 nm)	3.3721 (367.67 nm)

MNEI+Br	1.9975 (620.69 nm)	2.0676 (599.65 nm)	3.0886 (401.43 nm)	3.1088 (398.82)
MNEI+I	1.6083 (770.91 nm)	1.5128 (819.56 nm)	2.8209 (439.52 nm)	2.6780 (462.97 nm)

Table S9. Excited energies to CT_1 states of each complex at the several levels

CT_2	B3LYP		CAM-B3LYP	
	6-31G* / eV	6-31+G* / eV	6-31G*	6-31+G*
MNEI	–––––	–––––	–––––	–––––
MNEI+F	4.3666 (283.94 nm)	4.3941 (282.16 nm)	4.3849 (282.75 nm)	4.3144 (287.37 nm)
MNEI+Cl	3.7814 (327.88 nm)	3.8549 (321.62 nm)	4.3542 (284.75 nm)	4.2686 (290.45 nm)
MNEI+Br	3.6938 (335.65 nm)	3.6437 (340.27 nm)	4.3545 (284.72 nm)	4.2621 (290.90 nm)
MNEI+I	3.6510 (339.59 nm)	3.5215 (352.08 nm)	4.1547 (298.42 nm)	4.0320 (307.50 nm)

1

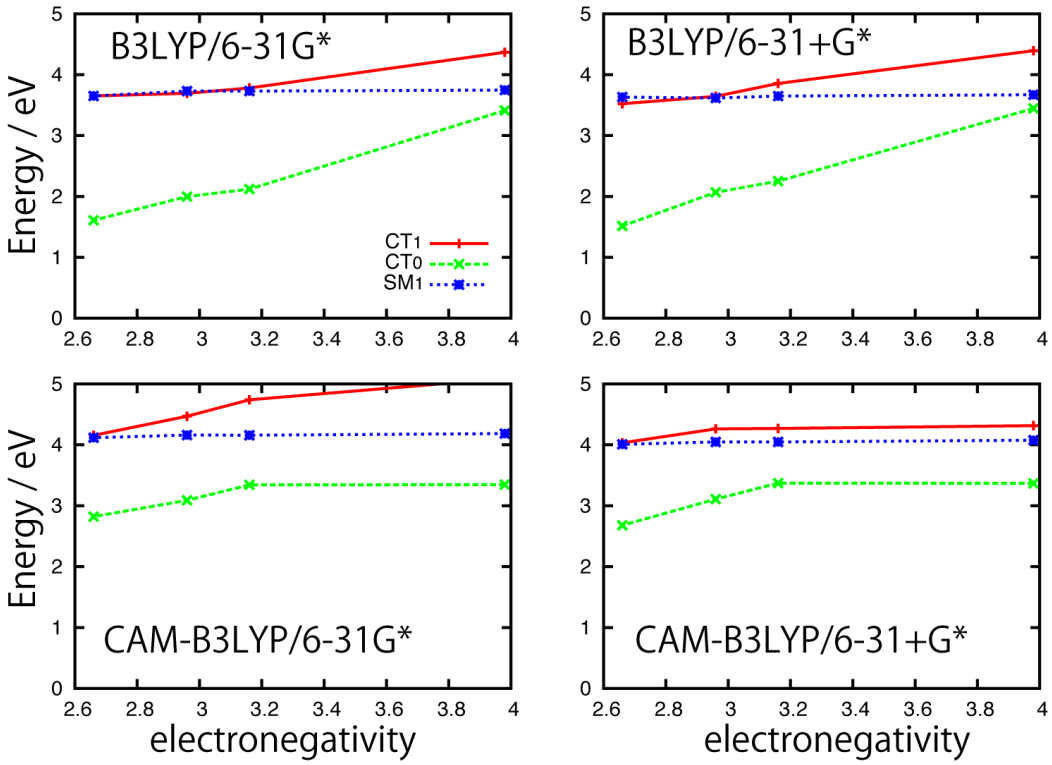

2

3 Figure S10. The CT_0, CT_1, SM_1 energies as the function of electronegativity. The qualitative

4 tendency, that is, the CT_1 state degenerates with the S_{M1} state while the electronegativity

5 decreases, is kept in each level.

6

7-7. Functional and basis set dependence in dissociated limitation.

Table S10. Energy (E_h) in each dissociated limitation of MNEI-X (X = F, Cl, Br, I)

	MNEI cation + X^-	MNEI neutral + X
X = I	-7930.06787468	-7930.08546005
X = Br	-3581.86865626	-3581.90439781
X = Cl	-1470.359550830	-1470.383721812
X = F	-1109.8614062831	-1109.9630160865

Table S11. Energy (E_h) in each dissociated limitation of MNEI-X (X = F, Cl, Br, I) at the B3LYP/6-31+G*

	MNEI cation + X^-	MNEI neutral + X
X = I		
X = Br	-3581.93603356	-3581.95550537
X = Cl	-1470.407576146	-1470.422128156
X = F	-1109.9925479053	-1110.0144248222

Table S12. Energy (E_h) in each dissociated limitation of MNEI-X (X = F, Cl, Br, I) at the CAM-B3LYP/6-31G*

	MNEI cation + X^-	MNEI neutral + X
X = I	-7929.79058660	-7929.80562477
X = Br	-3581.45213383	-3581.48498517
X = Cl	-1469.845858795	-1469.867247441

X = F	-1109.3250593684	-1109.4235151012

Table S13. Energy (E_h) in each dissociated limitation of MNEI-X (X = F, Cl, Br, I) at the CAM-B3LYP/6-31+G*

	MNEI cation + X^-	MNEI neutral + X
X = I	-7929.81498132	-7929.84249541
X = Br	-3581.51741356	-3581.53663531
X = Cl	-1469.892256737	-1469.906204048
X = F	-1109.4562476768	-1109.4761088887

References

S1. T. N. Konstantinova, P. Meallier and I. Grabchev, *Dyes Pigments*, 1993, **22**, 191-198.

S2. A. J. Arduengo, *Accounts Chem Res*, 1999, **32**, 913-921.

S3. E. Clementi, D. L. Raimondi and Reinhard.Wp, *J Chem Phys*, 1967, **47**, 1300-&.

S4. T. N. Konstantinova, P. Meallier and I. Grabchev, *Dyes Pigments*, 1993, **22**, 191-198.

S5. Gaussian 09, Revision D.01, M. J. Frisch, G. W. Trucks, H. B. Schlegel, G. E. Scuseria, M. A. Robb, J. R. Cheeseman, G. Scalmani, V. Barone, B. Mennucci, G. A. Petersson, H. Nakatsuji, M. Caricato, X. Li, H. P. Hratchian, A. F. Izmaylov, J. Bloino, G. Zheng, J. L. Sonnenberg, M. Hada, M. Ehara, K. Toyota, R. Fukuda, J. Hasegawa, M. Ishida, T. Nakajima, Y. Honda, O. Kitao, H. Nakai, T. Vreven, J. A. Montgomery, Jr., J. E. Peralta, F. Ogliaro, M. Bearpark, J. J. Heyd, E. Brothers, K. N. Kudin, V. N. Staroverov, R. Kobayashi, J. Normand, K. Raghavachari, A. Rendell, J. C. Burant, S. S. Iyengar, J. Tomasi, M. Cossi, N. Rega, J. M. Millam, M. Klene, J. E. Knox, J. B. Cross, V. Bakken, C. Adamo, J. Jaramillo, R. Gomperts, R. E. Stratmann, O. Yazyev, A. J. Austin, R. Cammi, C. Pomelli, J. W. Ochterski, R. L. Martin, K. Morokuma, V. G. Zakrzewski, G. A. Voth, P. Salvador, J. J. Dannenberg, S. Dapprich, A. D. Daniels, Ö. Farkas, J. B. Foresman, J. V. Ortiz, J. Cioslowski, and D. J. Fox, Gaussian, Inc., Wallingford CT, 2009.